

Prediction of Adenomyosis Diagnosis based on MRI

Connie Rees¹, Marloes van de Wiel¹, Joost Nederend¹, Aleida Huppelschoten¹, Massimo Mischi², Huib van Vliet¹, and Benedictus Schoot¹

¹Catharina Hospital

²Eindhoven University of Technology

February 22, 2024

Abstract

Study Objective: Development of a prediction tool for histopathological adenomyosis diagnosis after hysterectomy based on MRI and clinical parameters. **Design:** Single-centre retrospective cohort study **Setting:** Gynaecological department of a referral hospital from 2007-2022. **Population:** 296 women undergoing hysterectomy with preoperative pelvic MRI **Methods:** MRI's were retrospectively assessed for adenomyosis markers (junctional zone (JZ) parameters, high signal intensity foci (HSI) foci) in a blinded fashion. A multivariate regression model for histopathological adenomyosis diagnosis was developed based on MRI and clinical variables from univariate analysis with $p > 0.10$ and factors deemed clinically relevant. **Results:** 131/296 women (44.3%) had histopathological adenomyosis. Patients were of comparable age at hysterectomy, BMI and clinical symptoms, $p > 0.05$. Adenomyosis patients more often had undergone a curettage (22.1% vs. 8.9%, $p = 0.002$), a higher mean JZ thickness (9.40 vs. 8.35mm, $p < .001$), maximal JZ thickness (16.00 vs. 13.40mm, $p < .001$), mean JZ/myometrium ratio (0.56 vs. 0.49, $p = .040$), and JZ differential (8.60 vs. 8.15mm, $p = .003$). Presence of HSI foci was a strong predictor for adenomyosis (39.7% vs. 8.9%, $p < .001$). Based on the parameters age and BMI, history of curettage, dysmenorrhoea, abnormal uterine bleeding (AUB), mean JZ, JZ Differential ≥ 5 mm, JZ/myometrium ratio $> .40$, and presence of HSI Foci, a predictive model was created with a good Area Under the Curve (AUC) of .776. **Conclusions:** This is the first study to create a diagnostic tool based on MRI and clinical parameters for adenomyosis diagnosis. After sufficient external validation, this model could function as a useful clinical-decision making tool in women with suspected adenomyosis.

INTRODUCTION:

The golden standard to diagnose adenomyosis is histopathological after hysterectomy. Adenomyosis can also be diagnosed using Magnetic Resonance Imaging (MRI) ¹⁻³. Accurate diagnosis on MRI remains challenging as a consensus on diagnostic criteria is lacking⁴. Clinically, adenomyosis can be suspected based on symptoms (dysmenorrhoea, abnormal uterine bleeding (AUB) and infertility^{4,5}), but this can be difficult due to up to a third of patients being asymptomatic^{4,6}. Ultrasound (TVUS) diagnostic criteria do exist ⁷⁻⁹, but are dependent on experienced sonographers ¹⁰⁻¹². Furthermore TVUS is less reliable in cases of mild or atypical adenomyosis^{7,13}. Moreover, in cases with combined pathology (e.g. adenomyosis and fibroids, or adenomyosis and endometriosis) TVUS diagnosis can be extra challenging ⁷. In cases such as these, MRI can help lead to a more definitive diagnosis.

In the frequently associated condition endometriosis¹⁴, reported diagnostic delay is up to nine years^{15,16}. The diagnostic delay for adenomyosis is unknown. The mental and physical toll on women suffering from either of these conditions is considerable ¹⁷. Especially in women of fertile age, there is a need for an accurate diagnostic tool so that appropriate management can be implemented swiftly. Early diagnosis is clinically relevant even in mild cases, due to a potential for reproductive sequelae ⁵. Such a tool could also be used to predict certain clinical outcomes such as treatment response, or fertility outcomes.

There are a wide range of MRI parameters that can be used to characterise adenomyosis, such as junctional

zone (JZ) thickness, myometrial signal intensity and uterine size^{3,18}. Many of them have not been investigated for diagnostic accuracy, and little is likewise known about their correlation with clinical outcomes^{3,19}. Despite attempts to create (imaging-based) classification systems for adenomyosis^{20,21}, there exists no clinically applicable tool for prediction of adenomyosis diagnosis on MRI.

This study aims to create a prediction model for histopathological diagnosis of adenomyosis based on a combination of MRI parameters and clinical criteria prior to hysterectomy.

METHODS:

Study Objective:

To develop a multivariate prediction model for adenomyosis diagnosis on histopathology after hysterectomy based on MRI and clinical parameters.

Setting:

Gynaecological department of regional referral teaching hospital, the Catharina Hospital, in Eindhoven, the Netherlands

Design:

Single centre retrospective observational cohort study

Patient Selection and Eligibility:

Patients were selected through screening of electronic hospital patient records in Healthcare Information eXchange (HiX) (ChipSoft BV, Amsterdam, the Netherlands), based on electronic search queries in CTcue (CTcue BV, Amsterdam, the Netherlands). Relevant search terms are presented in Supplementary File A.

Women were eligible for inclusion if they underwent a hysterectomy due to benign pathology in our centre between 2007 and March 2022 and had pre-operative pelvic MRI available. Subjects were included regardless of symptoms. Subjects were excluded if: they did not have a pelvic MRI prior to hysterectomy, they had an unsuitable MRI protocol (see appendix B for further specification), they were post-menopausal (due to no longer active disease), had a gynaecological malignancy or if no pathology report available after hysterectomy. Patients were also excluded if they explicitly stated in their file that they did not want their information to be used for research purposes.

Outcomes:

The primary outcome assessed in this study is the histopathological diagnosis of adenomyosis after hysterectomy. Secondary outcomes include clinical and MRI parameters of included patients.

Histopathology Diagnosis:

Adenomyosis was diagnosed based on histopathology if endometrial glands were seen in the myometrium:

- At least one low power field from endomyometrial junction, (which is irregular), or
- 1 to 2.5 mm below basal layer of endometrium, or
- Deeper than 25% of the overall myometrial thickness

Local MRI Protocol:

All pelvic MRIs were carried out with either a 1.5T or 3T MRI system (Philips, Ingenia, the Netherlands). Local protocol included a T2-weighted turbo spin echo (T2-TSE) sequence in the sagittal, axial, and coronal planes, and a T1-weighted turbo spin echo (T1-TSE) sequence in the axial plane. A slice thickness of 3 millimetres was generally used, with variations ranging from 3-5 millimetres. All patients were pre-treated with an antispasmodic agent (1 mL of 20 mg/mL Buscopan?, Sanofi, Paris, France) intravenously or intramuscularly to minimise the effects of uterine and bowel peristalsis on image interpretation. Some patients

received multiple pelvic MRIs prior to hysterectomy. In those cases, the MRI closest to the hysterectomy was chosen for the assessment. See supplementary file B for full details.

MRI Assessment:

Two investigators (MvdW and CR) independently reviewed all pelvic MRIs for signs of adenomyosis blinded to the final histopathological diagnosis. Adenomyosis was suspected when one or more of the following features was present: (irregular) JZ >12mm, presence of myometrial high signal intensity (HSI) foci and/or asymmetric enlarged uterus (other than due to presence of leiomyoma's). Measurements were done using Spectra IDS7 version 21.1 (Linköping, Sweden). Table S1 shows an overview and definition of the parameters that were measured. Consensus was reached if there was a difference of <2mm. If discrepancies existed between the assessments of the two investigators, expertise was sought from a pelvic radiologist (J.N.). The researchers independently concluded whether an MRI adenomyosis diagnosis was suspected, after which the pathology report was consulted to review the conclusive histopathological diagnosis. The influence of uterine contractions on JZ measurements was minimised by confirming (maximal) JZ thickness in more than one imaging plane. In the case of bad quality MRIs, or extremely abnormal uteri affecting the ability for assessment, only those MRI parameters that could be reliably measured were assessed.

Data Management:

To store patient data, protected software, Research Manager (Research Manager, Deventer, the Netherlands), was used. Data pertaining to patients were given a pseudonymized study ID and could therefore not be traced back to the individual patient.

Data Analysis and Model Development

The study was conducted conform both the STROBE²² and the TRIPOD statements²³ (see supplementary files C and D for the appropriate checklists). All statistical analyses were conducted with IBM SPSS Statistics, version 28.0 (IBM Corp., Armonk, NY, USA). Flowcharts were created using Miro (Miro, Amsterdam, the Netherlands). Except for univariate logistic regression analysis, a p -value of <.05 was considered statistically significant for all variables.

Between-group differences were compared between patients with and without a histopathological adenomyosis diagnosis after hysterectomy. For clinical characteristics and primary MRI parameters, counts and frequencies were reported. For normally distributed continuous variables, means and standard deviations were calculated. For continuous variables that were not normally distributed, medians and inter-quartile ranges were given. To assess between-group differences for continuous variables, Student's t -Test and Mann-Whitney U test were used. For categorical variables, the Chi Squared test was used.

For all possible predictive factors, sensitivity, specificity, PPV, NPV, positive likelihood ratio (PLR), negative likelihood ratio (NLR), and accuracy were calculated. Potential threshold values of continuous variables were investigated using Receiver Operator Characteristics (ROC) curves and Area Under the Curve (AUC) to identify appropriate cut-off values, and to test the prognostic diagnostic potential for histopathological adenomyosis diagnosis.

For the development of the prediction model, the methodology as described by Grant et al.²⁴ and the TRIPOD guidelines were followed²³. For all individual potential predictors for a histopathological adenomyosis diagnosis, a univariate logistic regression analysis was first performed. The odds ratios (ORs) with their corresponding 95% confidence intervals (CIs) were reported. Missing values were dealt with by multiple imputation. Furthermore, interaction terms were used to test possible interaction between individual predictive factors. Tests for multicollinearity were performed as well to assess potential correlation between predictors. Individual variables were used for inclusion into the multivariate logistic regression model if they had a p -value <.10 in the univariate logistic regression analysis, or if they were considered clinically relevant, and if they had a high diagnostic performance (sensitivity/specificity >70% or AUC >0.70). Overfitting of the model was avoided by reducing the number of variables included in the model and by using shrinkage factors.

Model fit was further improved by including additional predictive power of continuous variables based on locally weighted smoothing (LOESS).

The final model was evaluated for discrimination and calibration performance. The AUC was obtained to discriminate between women with and without a histopathological adenomyosis diagnosis after hysterectomy. To assess the calibration of the predicted probabilities, and to show the relation between predicted and observed probabilities for the histopathological adenomyosis diagnosis, an observed to expected ratio was calculated and a Hosmer and Lemeshow Test was performed.

RESULTS:

Patient selection

296 women out of 1,139 potentially eligible women, were included for analysis. See figure S1 for detailed overview of the patient selection and exclusion procedure.

Patient characteristics

Table 1 presents patient characteristics of patients with and without a histopathological adenomyosis diagnosis. Out of 296 patients undergoing hysterectomy, 131 (44.2%) received adenomyosis diagnosis based on histopathology. 34.4% (45/131) patients had concomitant uterine fibroids, and 53.4% (70/131) had concomitant endometriosis (as diagnosed by MRI or laparoscopy). In general, age, Body Mass Index (BMI), medical history, and clinical symptoms were comparable between patients with and without adenomyosis ($p > .05$). However, patients with a histopathological diagnosis of adenomyosis more often had a history of curettage after miscarriage (22.1% vs. 8.9%, $p = .002$).

MRI characteristics

Table 2 presents primary MRI characteristics of patients with and without a histopathological diagnosis of adenomyosis. 21 patients were not assessed on MRI due to a poor quality of the MRI, or the inability of the researchers to identify the endometrium or the JZ (e.g. due to disruption of the normal uterine anatomy in patients with severe uterine fibroids). Furthermore, 52 MRIs were re-assessed and discussed with a third investigator due to discrepancies between the two researchers. Most discrepancies related to the presence of High Signal Intensity (HSI) foci ($n=31$) and individual JZ measurements (including JZ Max) ($n=15$) (see Table S2 for further details).

Significant differences between groups were found for mean JZ thickness, maximal JZ thickness, and JZ differential (JZ Diff) ($p < .001$, $< .001$, and $.003$, respectively). Similar differences were observed for the cut-offs of JZ [?]12 mm, JZ Diff [?]5 mm, and JZ to myometrium ratio (JZ/MYO) $> .4$ ($p = .004$, $.024$, and $.021$, respectively). Compared to patients without adenomyosis, the MRIs of patients with adenomyosis more often showed HSI foci (39.7% vs. 8.9%, $p < .001$). Figure 1 shows illustrative examples of these MRI features in patients with and without a histopathological diagnosis of adenomyosis.

Diagnostic accuracy

Table 3 presents the diagnostic accuracy of MRI in general and the individual potential predictors of adenomyosis. MRI overall had a sensitivity of 50.4%, a specificity of 66.9%, a PPV of 55.9%, a NPV of 61.8%, a positive LR of 1.5, and a negative LR of 0.7. The overall accuracy was 59.4%. A history of curettage showed an overall accuracy of 59.7%, with a sensitivity of 22.1%, a specificity of 91.1%, a PPV of 67.4%, a NPV 58.4%, a positive LR 2.5, and a NLR of 0.9. Additionally, AUB had a sensitivity of 94.2%, a specificity of 11.1%, a PPV of 47.9%, and a NPV of 68.8%. The positive LR of AUB was 1.1, negative LR 0.5, and overall accuracy 49.7%. A JZ Diff [?] 5 mm on MRI had an overall accuracy of 54.8%, with a sensitivity of 88.6%, a specificity of 22.0%, a PPV of 52.5%, a NPV of 66.7%, a positive LR of 1.1, and a negative LR of 0.5. The sensitivity of the presence of HSI foci was 40.3%, the specificity was 91.0%, the PPV was 48.4%, and the NPV was 52.6%. The positive LR was 4.8, the negative LR was 0.7, and the overall accuracy was 68.1%. Reader (CR and MvdW) detection versus initial radiologist diagnosis is shown in Table S3.

In tests for individual prognostic diagnostic potential using the ROC-curve, no continuous variables showed an AUC ≥ 0.7 . Highest AUCs were found for mean JZ thickness and JZ Max (AUC .624) (data not shown).

Prediction of histopathological adenomyosis

Table 4 presents the results of both univariate and multivariate logistic regression analysis. Univariate logistic regression analysis showed p-values $< .10$ for: age at MRI, history of curettage, mean JZ thickness, JZ Max, JZ Diff, JZ/MYO, mean uterine volume, JZ Max ≥ 12 mm, JZ Diff ≥ 5 mm, and the presence of HSI foci. The potential predictors showed no two-way interaction; however, mean JZ thickness, JZ Max, and JZ Diff did show multicollinearity. These variables were not included in the multivariate regression model to avoid overoptimism. Nevertheless, high diagnostic performance was found for dysmenorrhoea and AUB (sensitivity/specificity $> 70\%$). Additionally, due to clinical relevance, BMI was manually forced into the multivariate model. The final model included age at MRI, BMI, history of curettage, dysmenorrhoea, AUB, mean JZ thickness, JZ Diff ≥ 5 mm, JZ/MYO $> .40$, and the presence of HSI foci. In this model, mean JZ thickness, JZ/MYO $> .40$ and the presence of HSI foci reached statistical significance. Preference was given to variables with the most statistical significance in univariate analysis, and the number of included variables in the model was kept to a minimum. To further correct the model for overfitting, a shrinkage factor of .747 was applied. Since LOESS already showed a good model fit for the continuous variables of interest, no modifications were necessary. The formula for the final prediction model therefore is as follows:

1

Y =

$$1 + e^{-(-3.246 + (\text{age} \cdot .032) + (\text{BMI} \cdot .026) + (\text{history of curettage (yes=1 no=0)} \cdot .633) + (\text{dysmenorrhoea (yes=1 no=0)} \cdot .073) + (\text{AUB (yes=1 no=0)} \cdot .028) + (\text{mean JZ} \cdot .138) + (\text{JZ Diff} \geq 5 \text{ mm (yes=1 no=0)} \cdot .320) - (\text{JZ/MYO} > .04 \text{ (yes=1 no=0)} \cdot 1.226) + (\text{HSI Foci (yes=1 no=0)} \cdot 1.148))}$$

Discrimination performance evaluation of this prediction model showed an AUC of .776. A sub-analysis was conducted to assess whether the clinical query presented to the pathologist affected model diagnostic performance. The pathologist was directly asked to assess for the presence of adenomyosis in 142/296 patients. Model diagnostic performance did not improve significantly when adenomyosis was specifically evaluated for (data not shown).

Calibration performance evaluation showed an observed to expected ratio of 1.2, and the Hosmer and Lemeshow test that did not reach statistical significance ($p = .688$).

DISCUSSION:

Main Findings:

We assessed clinical and MRI parameters for their potential to predict histopathological adenomyosis diagnosis prior to hysterectomy. The resultant multivariate prediction model discriminates well between patients with and without adenomyosis (AUC 0.776). Five clinical characteristics: age at MRI, BMI, history of curettage, dysmenorrhoea, and AUB, and four primary MRI parameters: mean JZ thickness, JZ Diff ≥ 5 mm, JZ/MYO $> .40$, and the presence of HSI foci are included.

Strengths and Limitations:

This study has several strengths and limitations that merit consideration. A strength of our study is that two researchers independently reviewed all pelvic MRIs blinded to the histopathology outcome. Furthermore, the proposed model was built on data of 296 patients and data driven variable selection was avoided, along with corrections for potential overfitting. Additionally, the combination of both clinical and MRI parameters makes this model easily implementable into daily clinical practise.

The present study used broad inclusion criteria, which could be interpreted as both a strength and limitation. On the one hand, inclusion of patients with comorbidities like uterine fibroids might have prevented

an overestimation of diagnostic performance of the individual potential predictors. Alternatively, severe distortion of the uterus due to fibroids or endometriosis can limit the ability for objective assessment of all MRI parameters.

One limitation of the current study is that it was not possible to correct for the influence of the menstrual cycle on MRI parameters. Although it is known that JZ thickness changes during the menstrual cycle²⁵, cycle phase at time of MRI was not reported for most of our patients. Furthermore, the choice for histopathology after hysterectomy as a reference standard introduces an element of selection bias. Potentially, our group consisted of women with more severe adenomyosis and thus may have affected the general phenotype. The present study did not conduct a central review of pathology however, and (histological) adenomyosis severity was generally not reported in pathology reports. Therefore this remains hypothetical.

Interpretation of findings:

To the best of our knowledge, no comparable models for histopathological adenomyosis diagnosis based on MRI exist. Previous studies have investigated prediction of adenomyosis diagnosis based on ultrasound, with comparable accuracy^{9,11,26}. However, it is known that ultrasound diagnosis is highly operator dependent, with varying inter- and intra-observer variability^{8,27,28}. An MRI prediction model such as developed in our study thus has clinical value especially in cases where adenomyosis co-exists with other pathology (as was the case in the majority of our included patients), or is mild, or atypical.

The parameters ultimately included in this model are unsurprising when considering reported adenomyosis clinical presentation and aetiology. Dysmenorrhoea and AUB are the most frequently reported symptoms of adenomyosis^{4,29} and were thus logical (and statistically significant) additions to the model. Age at MRI was further included in the model due to the known physiological increase in JZ thickness with age^{25,30,31}. BMI was also manually entered into the model as, despite univariate analysis showing no significant association, increased body weight and obesity have been reported as strong risk factors for adenomyosis³².

History of curettage (after miscarriage) established itself to be an important predictor and was thus included in our model. It is debatable as to if curettage is a cause or a consequence of adenomyosis, as adenomyosis is often associated with risk of miscarriage⁵. Conversely, curettage as a risk factor for the development of adenomyosis could potentially be explained by iatrogenic trauma leading to the mechanical transport of endometrial cells into the myometrium^{33,34}.

None of the primary MRI parameters alone were sufficient to diagnose adenomyosis conclusively, which is in line with the literature (11). The presence of HSI foci emerged as the strongest predictor of the assessed MRI parameters ($p < .001$). Bazot et al. indeed described these foci as the only direct diagnostic criterion and almost pathognomonic for adenomyosis on MRI, although they are detected in only about half the cases (11).

In clinical practice, our model could be used to calculate the risk of adenomyosis in individual patients. For example, in a 31-year-old woman with a BMI of 19 kg/m², without history of curettage, with complaints of both dysmenorrhoea and AUB, and an MRI with mean JZ thickness of 8.3 millimetres, a JZ Diff <5 mm, a JZ/MYO >.40, but HSI Foci (Figure 1A), the probability of adenomyosis is 14.9%. In a 35-year-old woman with a BMI of 24 kg/m², without history of curettage, with complaints of both dysmenorrhoea and AUB, and an MRI with a mean JZ thickness of 24.6 millimetres, a JZ Diff [?]5 mm, a JZ/MYO >.40 and HSI Foci (Figure 1B), this probability increases to 90.3%.

CONCLUSION:

We present the first prediction model for histopathological adenomyosis diagnosis. In future, this tool can be useful for both patients and clinicians, with a potential to reduce morbidity and to contribute to shared decision making. Since patient management depends on several factors, such as age, symptoms, and comorbidity, the clinical use of the predicted risks from the proposed model should still be decided on an individual basis. Thus, before steps are made for use in clinical practise, external validation of the model is needed.

CONFLICTS OF INTEREST: None of the authors have any relevant conflicts of interest to disclose.

AUTHOR CONTRIBUTIONS:

CR, HvV and BC conceived and designed the study. MvdW and CR collected and analysed the data, and drafted the manuscript. JN gave access to crucial data and offered expertise in data collection and analysis of MRIs specifically. JN, AH and MM made critical contributions to the presentation, revision and interpretation of the final results, and approved the final version to be published. All authors concurred with the final version of this manuscript.

ETHICS APPROVAL:

This study was approved by the local medical ethical review board, with study number nWMO-2020.135. Informed consent was waived due to the retrospective study design.

REFERENCES:

1. Tellum T, Nygaard S, Lieng M. Noninvasive Diagnosis of Adenomyosis: A Structured Review and Meta-Analysis of Diagnostic Accuracy in Imaging. *J Minim Invasive Gynecol* [Internet]. 2019 Nov; Available from: <https://www.ncbi.nlm.nih.gov/pubmed/31712162>
2. Dueholm M, Hjorth IMD. Structured imaging technique in the gynecologic office for the diagnosis of abnormal uterine bleeding. *Best Pract Res Clin Obstet Gynaecol* [Internet]. 2017 Apr;40:23–43. Available from: <https://www.ncbi.nlm.nih.gov/pubmed/27818130>
3. Rees CO, Nederend J, Mischi M, van Vliet HAAM, Schoot BC. Objective measures of adenomyosis on MRI and their diagnostic accuracy—a systematic review & meta-analysis. *Acta Obstetrica et Gynecologica Scandinavica*. 2021.
4. Chapron C, Vannuccini S, Santulli P, Abrao MS, Carmona F, Fraser IS, et al. Diagnosing adenomyosis: An integrated clinical and imaging approach. *Hum Reprod Update*. 2020;
5. Horton J, Sterrenburg M, Lane S, Maheshwari A, Li TC, Cheong Y. Reproductive, obstetric, and perinatal outcomes of women with adenomyosis and endometriosis: A systematic review and meta-analysis. *Hum Reprod Update*. 2019;
6. Protopapas A, Grimbizis G, Athanasiou S, Loutradis D. Adenomyosis: Disease, uterine aging process leading to symptoms, or both? *Facts, Views Vis ObGyn* [Internet]. 2020 Aug 5 [cited 2022 Jun 28];12(2):91. Available from: </pmc/articles/PMC7431194/>
7. Van den Bosch T, Van Schoubroeck D. Ultrasound diagnosis of endometriosis and adenomyosis: State of the art. *Best Pract Res Clin Obstet Gynaecol* [Internet]. 2018 Aug;51:16–24. Available from: <https://www.ncbi.nlm.nih.gov/pubmed/29506961>
8. Van den Bosch T, de Bruijn AM, de Leeuw RA, Dueholm M, Exacoustos C, Valentin L, et al. Sonographic classification and reporting system for diagnosing adenomyosis. *Ultrasound in Obstetrics and Gynecology*. 2019.
9. Tellum T, Nygaard S, Skovholt EK, Qvigstad E, Lieng M. Development of a clinical prediction model for diagnosing adenomyosis. *Fertil Steril*. 2018 Oct 1;110(5):957-964.e3.
10. Bazot M, Cortez A, Darai E, Rouger J, Chopier J, Antoine JM, et al. Ultrasonography compared with magnetic resonance imaging for the diagnosis of adenomyosis: Correlation with histopathology. *Hum Reprod*. 2001;
11. Andres MP, Borrelli GM, Ribeiro J, Baracat EC, Abrao MS, Kho RM. Transvaginal Ultrasound for the Diagnosis of Adenomyosis: Systematic Review and Meta-Analysis. *J Minim Invasive Gynecol*. 2018 Feb 1;25(2):257–64.

12. Lazzeri L, Giovanni A Di, Exacoustos C, Tosti C, Pinzauti S, Malzoni M, et al. Preoperative and Post-operative Clinical and Transvaginal Ultrasound Findings of Adenomyosis in Patients With Deep Infiltrating Endometriosis.
13. Valentini AL, Speca S, Gui B, Soglia BG, Micco M, Bonomo L. Adenomyosis: From the sign to the diagnosis. Imaging, diagnostic pitfalls and differential diagnosis: A pictorial review. *Radiologia Medica*. 2011.
14. Gonzales M, Accardo De Matos L, Orlando Da Costa Goncalves M, Blasbalg R, Joao A, Dias J, et al. Patients with adenomyosis are more likely to have deep endometriosis.
15. Agarwal SK, Chapron C, Giudice LC, Laufer MR, Leyland N, Missmer SA, et al. Clinical diagnosis of endometriosis: a call to action. *Am J Obstet Gynecol*. 2019 Apr 1;220(4):354.e1-354.e12.
16. Staal AHJ, Van Der Zanden M, Nap AW. Diagnostic Delay of Endometriosis in the Netherlands. *Gynecol Obstet Invest*. 2016 Jul 1;81(4):321–4.
17. Gambadauro P, Carli V, Hadlaczky G. Depressive symptoms among women with endometriosis: a systematic review and meta-analysis. Vol. 220, *American Journal of Obstetrics and Gynecology*. Mosby Inc.; 2019. p. 230–41.
18. Agostinho L, Cruz R, Osorio F, Alves J, Setubal A, Guerra A. MRI for adenomyosis: a pictorial review. *Insights Imaging* [Internet]. 2017 Dec;8(6):549–56. Available from: <https://www.ncbi.nlm.nih.gov/pubmed/28980163>
19. Munro MG. Classification Systems for Adenomyosis. *J Minim Invasive Gynecol* [Internet]. 2019 Nov; Available from: <https://www.ncbi.nlm.nih.gov/pubmed/31785418>
20. Kishi Y, Suginami H, Kuramori R, Yabuta M, Suginami R, Taniguchi F. Four subtypes of adenomyosis assessed by magnetic resonance imaging and their specification. *Am J Obstet Gynecol* [Internet]. 2012 Aug;207(2):114.e1-7. Available from: <https://www.ncbi.nlm.nih.gov/pubmed/22840719>
21. Kobayashi H, Matsubara S. A Classification Proposal for Adenomyosis Based on Magnetic Resonance Imaging. *Gynecol Obstet Invest*. 2020;85(2):118–26.
22. Von Elm E, Altman DG, Egger M, Pocock SJ, Gotsche PC, Vandenbroucke JP. The Strengthening the Reporting of Observational Studies in Epidemiology (STROBE) Statement: guidelines for reporting observational studies*. *Bull World Health Organ* [Internet]. 2007 [cited 2022 Apr 11];85(11):867–72. Available from: <http://www.strobe-statement.org>
23. Collins GS, Reitsma JB, Altman DG, Moons KGM. Transparent Reporting of a multivariable prediction model for Individual Prognosis Or Diagnosis (TRIPOD): the TRIPOD Statement. 2015; Available from: <http://www.annals.org>
24. Grant SW, Collins GS, Nashef SAM. Statistical Primer: developing and validating a risk prediction model +. *Cardiothorac Surg* [Internet]. 2018;54:203–11. Available from: <https://academic.oup.com/ejcts/article/54/2/203/4993384>
25. Meylaerts LJ, Wijnen L, Grieten M, Palmers Y, Ombelet W, Vandersteen M. Junctional zone thickness in young nulliparous women according to menstrual cycle and hormonal contraception use. *Reprod Biomed Online*. 2017;
26. Champaneria R, Abedin P, Daniels J, Balogun M, Khan KS. Ultrasound scan and magnetic resonance imaging for the diagnosis of adenomyosis: Systematic review comparing test accuracy. *Acta Obstetrica et Gynecologica Scandinavica*. 2010.
27. Rasmussen CK, Hansen ES, Dueholm M. Inter-rater agreement in the diagnosis of adenomyosis by 2- and 3-dimensional transvaginal ultrasonography. *J Ultrasound Med* [Internet]. 2019 Mar 1 [cited 2022 Aug 1];38(3):657–66. Available from: <https://onlinelibrary.wiley.com/doi/full/10.1002/jum.14735>

28. Habiba M, Gordts S, Bazot M, Brosens I, Benagiano G. Exploring the challenges for a new classification of adenomyosis. *Reprod Biomed Online*. 2020 Apr 1;40(4):569–81.

29. Aleksandrovykh V, Basta P, Gil K. Current facts constituting an understanding of the nature of adenomyosis. *Advances in Clinical and Experimental Medicine*. 2019.

30. Maubon A, Faury A, Kapella M, Pouquet M, Piver P. Uterine junctional zone at magnetic resonance imaging: A predictor of in vitro fertilization implantation failure. *J Obstet Gynaecol Res*. 2010;

31. Hauth EAM, Jaeger HJ, Libera H, Lange S, Forsting M. MR imaging of the uterus and cervix in healthy women: determination of normal values. *Eur Radiol [Internet]*. 2007 Mar;17(3):734–42. Available from: <https://www.ncbi.nlm.nih.gov/pubmed/16703306>

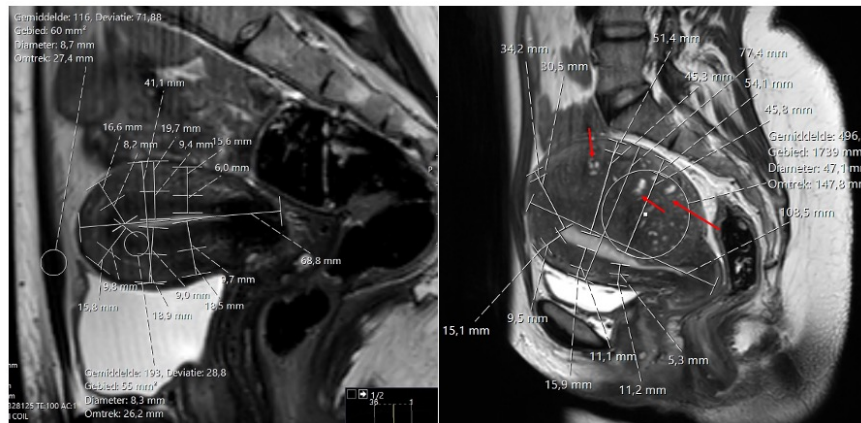
32. Templeman C, Marshall SF, Ursin G, Horn-Ross PL, Clarke CA, Allen M, et al. Adenomyosis and endometriosis in the California Teachers Study. *Fertil Steril*. 2008 Aug 1;90(2):415–24.

33. Guo SW. The Pathogenesis of Adenomyosis vis-a-vis Endometriosis. *J Clin Med [Internet]*. 2020 Feb 10 [cited 2020 Aug 3];9(2):485. Available from: <https://www.mdpi.com/2077-0383/9/2/485>

34. Leyendecker G, Bilgicyildirim A, Inacker M, Stalf T, Huppert P, Mall G, et al. Adenomyosis and endometriosis. Re-visiting their association and further insights into the mechanisms of auto-traumatisation. An MRI study. *Arch Gynecol Obstet*. 2015;

FIGURE LEGENDS:

Figure 1. Illustrative examples of MRI’s of two included patients. **A.** MRI measurements in a patient without histopathological diagnosis of adenomyosis. Mean JZ thickness was 8.7mm (<12mm), JZ Max was 9.8 mm (<12 mm), and JZ Diff was 3.8mm (<5 mm). JZ/MYO was .50 (>.40), and HSI foci were not present. **B.** MRI measurements in a patient with histopathological diagnosis of adenomyosis. Mean JZ thickness was 24.6 mm ([?]12 mm), JZ Max was 45.8 mm ([?]12 mm), and JZ Diff was 40.5 mm ([?]5mm). JZ/MYO was 0.74 (>.40), and HSI foci were present (red arrows).



Hosted file

Table 1.docx available at <https://authorea.com/users/500765/articles/581469-prediction-of-adenomyosis-diagnosis-based-on-mri>

Hosted file

Table 2.docx available at <https://authorea.com/users/500765/articles/581469-prediction-of-adenomyosis-diagnosis-based-on-mri>

Hosted file

Table 3.docx available at <https://authorea.com/users/500765/articles/581469-prediction-of-adenomyosis-diagnosis-based-on-mri>

Hosted file

Table 4.docx available at <https://authorea.com/users/500765/articles/581469-prediction-of-adenomyosis-diagnosis-based-on-mri>